

A Novel Clustering-Based Algorithm for Continuous and Non-invasive Cuff-Less Blood Pressure Estimation

Ali Farki,¹ Reza Baradaran Kazemzadeh,¹ and Elham Akhondzadeh Noughabi¹

¹Department of Information Technology Engineering, Industrial and Systems Engineering Faculty, Tarbiat Modares University, Tehran, Iran

Correspondence should be addressed to Ali Farki; Alifarki@modares.ac.ir

Abstract

Continuous blood pressure (BP) measurements can reflect a body's response to diseases and serve as a predictor of cardiovascular and other health conditions. While current cuff-based BP measurement methods are incapable of providing continuous BP readings, invasive BP monitoring methods also tend to cause patient dissatisfaction and can potentially cause infection. In this research, we developed a method for estimating blood pressure based on the features extracted from Electrocardiogram (ECG) and Photoplethysmogram (PPG) signals and the Arterial Blood Pressure (ABP) data. The vector of features extracted from the preprocessed ECG and PPG signals is used in this approach, which include Pulse Transit Time (PTT), PPG Intensity Ratio (PIR), and Heart Rate (HR), as the input of a clustering algorithm and then developing separate regression models like Random Forest Regression, Gradient Boosting Regression, and Multilayer Perceptron Regression algorithms for each resulting cluster. We evaluated and compared the findings to create the model with the highest accuracy by applying the clustering approach and identifying the optimal number of clusters, and eventually the acceptable prediction model. The paper compares the results obtained with and without this clustering. The results show that the proposed clustering approach helps obtain more accurate estimates of Systolic Blood Pressure (SBP) and Diastolic Blood Pressure (DBP). Given the inconsistency, high dispersion, and multitude of trends in the datasets for different features, using the clustering approach improved the estimation accuracy by 50-60%.

1. Introduction

Blood pressure (BP) is one of the most important health indicators and can be used to diagnose various diseases. BP measurement techniques can be broken down into two categories of Invasive methods and Non-invasive methods. While the invasive approach tends to provide more accurate BP readings, it has some drawbacks and limitations. The World Health Organization has issued reports on the subject that each year, 9.4 million people die from excessive blood pressure around the world (hypertension), and roughly 30% of all men and 25% of all women suffer from this condition[1]. After diabetes, hypertension is the second leading cause of cardiovascular disease, but it also tends to be asymptomatic, so it has been called the silent killer. As one of the vital signs, blood pressure needs to be regularly controlled. In many clinical settings, BP monitoring needs to be constant, especially if the patient is old or is in the intensive care unit (ICU). Regular BP monitoring can also help prevent stroke, heart attack, and heart failure[2]–[4]. Unfortunately, most people with hypertension are unaware of

their condition and how it harms their internal organs like the brain, eyes, and kidneys over time.

As mentioned earlier, there are two types of blood pressure measurement methods: Invasive and Non-Invasive. In Invasive Blood Pressure (IBP) monitoring, measurements are done by a sensor or cannula needle inserted in a blood vessel. This method can provide continuous accurate BP information but has drawbacks such as vessel blockage and potential area infection[5]. Non-invasive Blood Pressure (NIBP) monitoring methods can be classified into two categories: 1- the auditory methods and 2- the methods based on vital signals. The auditory method is the common BP measurement method which involves wrapping a cuff around the arm. Naturally, this method measures the blood pressure at one instant and cannot provide continuous BP readings. Also, using this method multiple consecutively leads to patient dissatisfaction[6]. Given the limitations of direct BP measurement methods, several indirect methods have also been developed for this purpose. As of this writing, researchers have not found a consistent relationship between Blood Pressure and Electrocardiogram and Photoplethysmogram signals, so that blood pressure can not be reliably obtained from these signals. However, there are indeed some relationships between blood pressure and the features extracted from these signals[7], [8]. Therefore, these features can be used to create prediction models for BP estimates using data analysis methods and technologies. In the non-invasive and cuff-less BP estimation method, we first extract a vector of physiological features from ECG and PPG signals and then develop a regression model for BP estimation with these features used as input[9], [10]. The greatest weakness of non-invasive cuff-less methods compared to other BP measurement methods is their lower accuracy, which can be somewhat improved by using a combination of different features and different machine learning and data mining methods. This paper introduces an algorithm for accurate cuff-less continuous BP estimation based on ECG and PPG signals. The first phase of this BP estimation is feature extraction. In this phase, the goal is to find the features in the person's vital signals that can be directly linked to their blood pressure.

The Pulse Transit Time (PTT), which is the time it takes for the arterial pulse wave to move from the aortic valve to the peripheral artery, is a typical approach to make continuous BP measurements. In other words, The time difference between the R-peak of the ECG signal and a reference point on the PPG signal of the corresponding pulse wave is referred to as the PTT[11]. The heart of this strategy is the notion of pulse wave velocity (PWV), which is obtained from the Moens-Korteweg equation (MK) [12]:

$$PWV = \sqrt{\frac{Eh}{d}} \quad (1)$$

In this equation, E is the elastic modulus of the arterial wall, h is the thickness of the wall, ρ is blood density, and d is the vessel radius. The following formula shows how PWV is inversely correlated to PTT[13]:

$$PWV = \frac{K}{PTT} \quad (2)$$

The distance between the heart and the reference peripheral (e.g., the fingertip) site is denoted by the K . The use of PWV leads to obtaining a more accurate PTT but requires parameters such as the person's physical characteristics[2], [14]–[16].

The ECG and PPG can derive the PTT features by taking the second derivative of the PPG or SDPPG signal. PTT indicates for the time interval between the peak of an ECG signal and a PPG signal reference point or the peak of a cycle in the SDPPG signal [10]. Unfortunately, PTT-based BP estimation alone is not accurate enough to be used for continuous cuff-less BP measurement in clinical settings[15]. However, this accuracy can be improved by the use of new BP-related features. One of the features that can increase the estimation accuracy of the regression model is Heart Rate (HR), as several studies have shown an improvement in the results after combining this feature with PTT [9]. Since the behavior of blood flow in vessels depends on various factors, PPG will also be a good signal to improve the results of BP estimation. This improvement can be made by combining PTT with several different features of PPG, one of which is the PPG Intensity Ratio (PIR).

In theory, changes in arterial diameter, Δd , could be reflected by PIR throughout one cardiac cycle from systole to diastole. Moreover, there is an exponential relationship between PIR and Δd that is shown by this expression[15], [17]:

$$PIR = e^{\alpha \Delta d} \quad (3)$$

Essentially, PIR has been defined as the maximum to minimum ratio of the amplitude of a PPG waveform. I_H is the peak point of a PPG cycle or maximum amplitude, and I_L is the bottommost point of a PPG cycle or minimum amplitude where α is a constant that is associated with the optical absorption coefficient in the light path. Physiologically, four variables largely influence BP, including cardiac output, arterial compliance, blood volume, and peripheral resistance. PTT could be used to evaluate arterial compliance because it has been proposed to be one of the indices of arterial stiffness[15], [18]. Moreover, there may be a relationship between cardiac output and PTT via the heart rate. Considering blood volume and peripheral resistance, changing the arterial diameter has been regarded as a main source to be evaluated by PIR that has been already illustrated. Therefore, BP changes could be directly captured by PIR and PTT employed to estimate BP[15].

The features used in this study are PTT, PIR, and HR, which are independent variables. Systolic Blood Pressure (SBP) and Diastolic Blood Pressure (DBP) are the dependent variables. After extracting these features, we developed several models based on regression on the data, but these models were found to be not sufficiently accurate because of the inconsistency and multitude of trends in the data for different features and the high dispersion of feature values. Thus, we clustered the data and developed a regression model for each cluster, and then obtained a final estimate by averaging the outputs of these models with attention to the number of samples in each cluster.

Figure 1 describes the block diagram of the process of BP estimation with the proposed method:

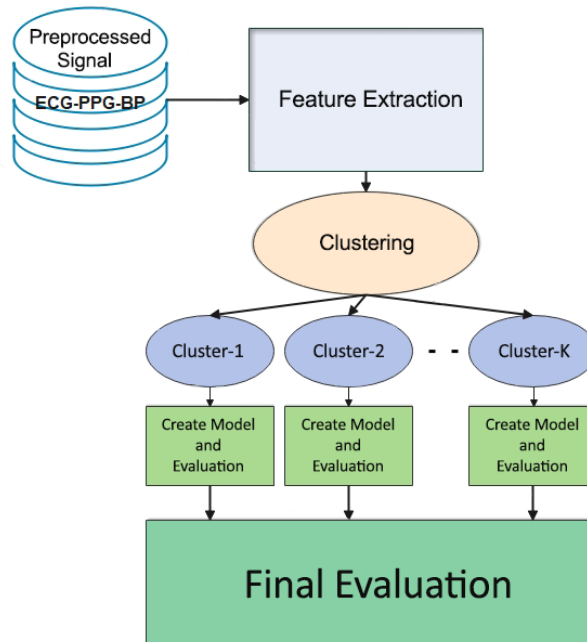


Figure 1. Cuff-less BP estimator with clustering block diagram

2. Materials and Methods

2.1 Dataset. The MIMIC-II (Multiparameter Intelligent Monitoring in Intensive Care) dataset from the Physionet website was used in this research. This dataset contains 12,000 records of vital signals captured from people admitted to American medical centers and hospitals. The signals of this dataset include ECG, PPG, and Arterial Blood Pressure (ABP) at a sampling rate of 125Hz [11]. A preprocessed and cleaned version of this dataset is publically available on the Kaggle website [14].

2.2. Features extraction. Figure 2 depicts the extraction process of PIR and PTT. Now, PTT represents the time between the peak of the second derivative of SDPPG or PPG wave in the cardiac cycle and the peak of the ECG wave. As mentioned earlier, PIR has been proposed to be the ratio of minimum amplitude (IL) to maximum amplitude (IL) of a PPG signal in the cardiac cycle[10], [15], [17].

The peak-to-peak time period of PPG or ECG data may be used to calculate HR or Heart Rate. In this study, we used the ECG signal for this purpose[9], [16]. The maximum and minimum amplitudes of the ABP signal were used to calculate Bpmin and Bpmax.

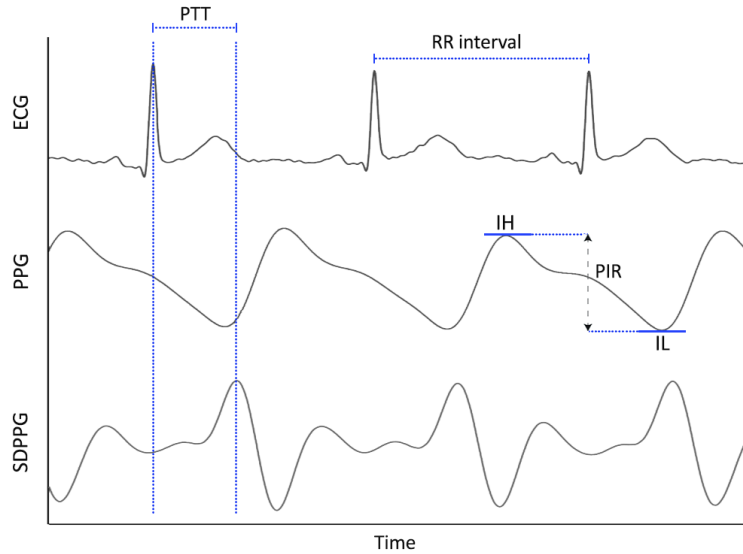


Figure 2 . Computation of the ratio of photoplethysmogram (PPG) intensity (PIR) and pulse transit time (PTT). Here, IH refers to the PPG peak intensity, SDPPG the second derivative of PPG, and finally IL valley intensity

2.3 Clustering and regression models

2.3.1 Clustering. There are several methods and algorithms for dividing a set of items into identical or highly similar clusters. The k-means algorithm is one of the simplest and most popular clustering algorithms used in data mining and unsupervised machine learning.

In multivariate clustering, it is typically needed to use multiple features of items to cluster them, which raises the question of what distance functions to use for this purpose. In any case, what is important in this clustering is the way we measure the degree of similarity or dissimilarity between data samples.

The goal of the clustering operation is to form clusters so that the distance between items in each cluster is minimal. In contrast, if the similarity of items is measured by a similarity function, the goal will be to form clusters so as to maximize the value of that function for each cluster. Given the inconsistency and multitude of trends in the data for different features and the high dispersion of feature values, we tried to first obtain clusters of data or independent variables. This was done by assessing the appropriateness of the number of clusters based on the silhouette value, and ultimately using the values of the independent variable in each cluster as the input of the regression model.

2.3.2 Random forest regression. Random Forest is an easy-to-use machine learning algorithm that tends to provide excellent results even without the adjustment of its meta-parameters. Thanks to its simplicity, this algorithm is one of the machine learning algorithms that are widely used for both classification and regression.

Random Forest falls in the category of supervised machine learning algorithms. As the name implies, this algorithm builds a random forest made of a group of decision trees. This is often done by the method known as bagging, the basic idea is to use a combination of learning models to reach better results. Simply put, Random Forest builds several decision trees and merges them to make more accurate and consistent predictions [19].

2.3.3 Gradient boosting regression. Gradient boosting is a classification and regression machine learning algorithm, which builds a prediction model using an ensemble of weak models. The goal of almost all machine learning algorithms is to minimize a defined loss function during the learning process. The constructed model needs to be updated such that the value of the loss function value approaches zero and the predicted values approach the observed values as much as possible.

The core idea of the gradient boosting algorithm is to make stronger models by combining weaker models in an iterative process.

Here, it is necessary to first describe how boosting models are created. To build boosting models, we first perform a sampling with replacement in which samples have a fixed weight in the selection probability calculations. After building a model with these samples, the samples that have produced the highest errors are returned to the sample pool and the sample selection probabilities for the next iteration of modeling are updated according to the error of each sample, which also ensures that the models properly cover the entire solution space. In the end, an ensemble of all models made through this process is created. The figure below shows the pseudocode of the boosting model construction process.

In gradient boosting regression, we first construct a regression tree model for the samples and measure the error of this model, i.e. the difference between the observed values and its predictions. We then build a new model for the data that the previous model have predicted incorrectly and recalculate the error. Next, we combine the new model with the previous one and update the ensemble. These steps are repeated until the sum of errors approaches a fixed value or the model becomes overfit [20].

2.3.4 Deep Multilayer Perceptron. MLP has been considered one of the supervised learning algorithms for learning a function $f(\cdot) = R^m \rightarrow R^o$ via training on a data-set so that \mathbf{m} and \mathbf{o} represent the number of dimensions for input and output, respectively.

According to the target \mathbf{y} and a collection of features $X = x_1, x_2, \dots, x_m$, MLP is capable of learning a nonlinear function approximator for regression and or classification. In fact, there is a difference between it and logistic regression because one or more nonlinear layers, known as hidden layers, may exist between the output and input layers. In addition, the leftmost layer that is also called input layer contains a set of neurons $\{x_i | x_1, x_2, \dots, x_m\}$ implying the input features. All neuron in the hidden layer transform values from the , previous layer with a weighted linear summation $\omega_1 x_1 + \omega_2 x_2 + \dots + \omega_m x_m$ and then a nonlinear activation $g(\cdot): R \rightarrow R$ such as the hyperbolic tan function.

2.4 Model evaluation

In this study, the modeling results are assessed in terms of Root Mean Square Error (RMSE) and Mean Absolute Error (MAE). Provided in the following is a description of these model evaluation criteria. The root mean square error (RMSE) quantifies how far the model's or statistical estimator's predicted values differ from the observed values. RMSE is an excellent measure for evaluating the prediction error of a model for a given dataset. This metric is basically the standard deviation of the difference between expected and observed values, as shown below:

$$RMSE = \sqrt{\frac{1}{n} \sum_{j=1}^n (y - \hat{y})^2} \quad (4)$$

As many have pointed out, because of using the square root of the mean square error, RMSE is not as biased as other measures and is very suitable for medical and bioinformatics problems that are solved by regression. The other error measure used in this study is MAE. MAE measures the difference between predicted and observed values without considering the direction of this difference. Therefore, what is important for MAE is the magnitude of error in estimations not whether they have been overestimates or underestimates. In statistical discussions, this measure is sometimes referred to as L1 Loss. Mathematically, MAE is the average absolute difference between predicted and observed value as formulated below:

$$MAE = \frac{\sum |y_i - \hat{y}_i|}{n} \quad (5)$$

3.Results

First, the data and the extracted features were visualized and the correlation between the features was measured. A very important section of creation regression model is the preparation of data, which in this study involved a scaling operation. This phase is very important because it affects how much time it takes to construct the regression model and the length of the convergence process. Next, we developed several machine learning regression models , including random forest regression, gradient boosting regression, and multilayer perceptron regression and evaluated the model outputs by different criteria. The next step was to implement the main approach of the study, that is, to cluster the extracted data or features and variables while using the silhouette value to determine the best number of clusters and then develop a model for each cluster with the regression algorithms mentioned above. the model outputs were compiled by weighted averaging ,and the final results were compared in terms of different measures to identify the best regression model.

Figure 3 shows the histogram and scatter diagram of PTT, PIR, BPPMIN, and BPPMAX. We used the scatter diagram to create a graphical representation of the relationship between independent and dependent features and we plotted a density diagram to gain an overview of the distribution of values for each feature.

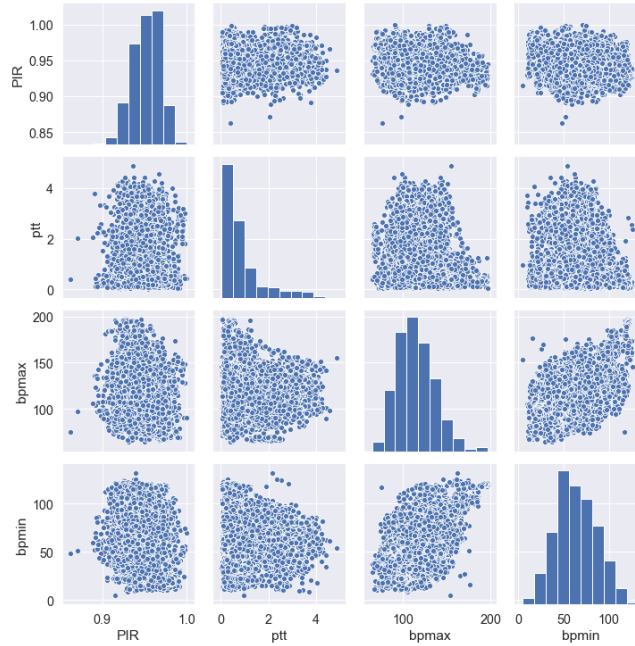


Figure 3 .histogram and scatter diagram of the features PTT, PIR, Bpmin, and Bpmax.

The next step was to obtain and examine the results of the machine learning regression models described in the previous sections. In this step, the machine learning models were developed with the features PTT, PIR, HR as independent variables (input) and bmin and bmax as dependent variables (output). First, we developed the model by regression on the entire data using random forest regression, gradient boosting regression, and multilayer perceptron regression. The results of this process are presented in Table 1. It should be noted that in all steps, the regression models were evaluated in terms of RMSE and MAE.

TABLE 1 COMPARISON OF THE PERFORMANCE WITHOUT CLUSTERING AND REGRESSION ALGORITHMS

Learner/Performance	Systolic Blood Pressure (mmHg)		Diastolic Blood Pressure (mmHg)	
	MAE	RMSE	MAE	RMSE
Random Forest Regression	7.426	12.250	7.410	12.110
Gradient Boosting Regression	6.367	10.395	6.276	10.221
MultiLayer Perceptron Regression	9.422	14.120	9.323	14.099

We utilized the k-means method to cluster the data using the Silhouette criteria to identify the optimal number of clusters, given the inconsistency and variety of trends in the data for different features. Figure 4 shows the cohesion and dispersion of data in one of the clusters extracted from the data.

Next, we used random forest regression, gradient boosting regression, and multilayer perceptron regression algorithms to develop a separate model for each cluster. The model error for each cluster was then determined in terms of RMSE and MAE. Finally, the total error of the model for all clusters was determined by weighted averaging. Finally, the error rate for the whole data and the total error rate are also provided. The results of the proposed clustering-based approach are presented in Table 2.

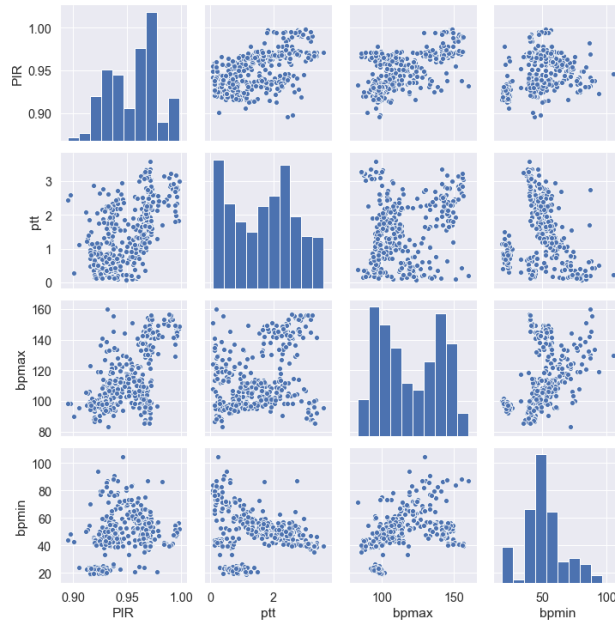


Figure 4 .histogram and scatter diagram of the features PTT, PIR, BPMIN, and BPMAX in one of the clusters

TABLE 2. COMPARISON OF THE PERFORMANCE WITH CLUSTERING AND REGRESSION ALGORITHMS

Learner/Performance	Cluster	Count of data per cluster	Systolic Blood Pressure (mmHg)		Diastolic Blood Pressure (mmHg)	
			MAE	RMSE	MAE	RMSE
Random Forest Regression	Cluster1	6282	3.407	5.830	3.250	5.698
	Cluster2	6276	3.468	5.724	3.038	5.136
	Cluster3	3355	3.521	5.586	2.813	5.408
	Cluster4	8300	3.396	5.500	2.870	4.852
	Cluster5	2390	2.434	4.567	2.677	4.879
	Total	26603	3.344	5.557	2.974	5.191
Gradient Boosting Regression	Cluster1	6282	2.644	5.841	2.486	5.648
	Cluster2	6276	2.781	5.694	2.468	5.232
	Cluster3	3355	2.533	6.123	2.003	5.491
	Cluster4	8300	2.610	5.522	2.161	4.675
	Cluster5	2390	1.643	4.709	1.504	4.467
	Total	26603	2.561	5.635	2.231	5.012
MultiLayer Perceptron Regression	Cluster1	6282	5.230	8.244	4.896	7.262
	Cluster2	6276	5.340	8.754	5.263	8.956
	Cluster3	3355	6.235	9.523	6.094	8.852
	Cluster4	8300	7.261	11.920	6.288	9.003
	Cluster5	2390	4.326	8.156	4.160	6.875
	Total	26603	5.937	9.664	5.501	8.370

4. Discussion

An important point regarding the MIMIC-II dataset is that it comprises data collected from ICUs from older patients under the influence of medication, which all affect the extracted features and ultimately the accuracy of BP estimation. Other signals, like as BCG and SCG, might possibly create more precise BP predictions, especially when used for proximal time reference[21]. Apart from vital signals, there are various parameters, such as age, weight, and height, that may be combined with vital signal attributes to generate even higher accuracies[9]. However, the goal of this study was to provide a method capable of delivering results irrespective of the data quality. While the feature extraction procedure used in this study was derived from the studies carried out by [15] and [16], it led to considerably better results than those achieved in these two studies. Table 3 makes a comparison between the results of this study and recent similar papers, previously published in journals and their methodology.

Table 3 COMPARISON WITH OTHER WORKS

Studies	Method	Machine learning comparison (DBP)		Machine learning comparison (SBP)	
		MAE	RMSE	MAE	RMSE
Our Proposed Method	Clustering & Gradient Boosting Regression	2.23	5.01	2.56	5.63
Our Proposed Method	Gradient Boosting Regression without Clustering	6.27	10.22	6.36	10.39
[16]	SVM	6.34	-	12.38	-
[9]	Adaboosting	5.35	-	11.17	-
[13]	MLR	2.82	-	2.83	-
[22]	Lstm & perceptron	-	6.49	-	7.86
[23]	Multi sensor features	4.54	-	6.13	-
[24]	PPG+CNN-Regression	3.45	-	5.73	-
[15]	PTT+PIR+ Nonlinear Regression	3.18	-	4.09	-
[25]	-	3.27	-	4.46	-
[26]	(PPG+ECG)	4.44	-	4.71	-
[27]	SVM	3.36	-	11.86	-
[28]	MLP	4.96	-	5.46	-
[29]	ECG: wrist & foot PPG: finger	4.4	-	6.0	-
[30]	ANN with 15 hidden neurons	-	-	3.03	-
[31]	PTT & PIR,Regression-MARS	4.86	-	7.83	-
[32]	AutoML(TPOT)	4.19	-	6.52	-
[33]	ANN	2.21±2.09	-	3.80±3.46	-
[34]	DNN	6.88	-	9.43	-
[35]	Res-LSTM	4.61	-	7.10	-
[36]	LSTM-base autoencoder	4.05	-	2.41	-

5. Conclusion and future works

This study developed a new clustering-based algorithm to improve the accuracy of the blood pressure estimation, which uses the K-means algorithm for Clustering extracted features and random forest regression algorithm, gradient boosting regression algorithm, and multilayer perceptron regression algorithm to estimate Systolic Blood Pressure (SBP) and Diastolic Blood Pressure (DBP) in each cluster. The results showed that, according to high dispersion and the multitude of trends in the data and extracted features, the clustering algorithm can increase the prediction accuracy by 50-60 % for each model. Overall, it can be concluded that since previous works have chosen not to deal with high dispersion and multitude of trends in the data before developing their learning models, it is indeed possible to reach considerably better prediction results by applying a clustering algorithm to the extracted data and then building a separate model for each cluster. In future works, we hope to develop a method for real-time feature extraction and sample clustering and ultimately create a real-time procedure for receiving vital signals such as ECG and PPG from thousands of people, performing feature extraction and signal processing, clustering the data, and producing BP estimates with the least possible delay and the highest possible accuracy; a task that will require using Big Data related platforms, tools, and algorithms.

Data Availability

The data for this study originated from PhysioNet and the well-known MIMIC-II database, however a preprocessed dataset from the MIMIC-II database is available at <https://www.kaggle.com/mkachuee/BloodPressureDataset>, which we utilized.

Conflicts of Interest

The authors declare that they have no conflicts of interest.

References

- [1] World Health Organization, *World health statistics 2015*. World Health Organization, 2015.
- [2] C. Poon and Y. Zhang, "Cuff-less and noninvasive measurements of arterial blood pressure by pulse transit time," 2006, pp. 5877–5880.
- [3] M. Liu, L.-M. Po, and H. Fu, "Cuffless blood pressure estimation based on photoplethysmography signal and its second derivative," *Int. J. Comput. Theory Eng.*, vol. 9, no. 3, Art. no. 3, 2017.
- [4] M. Shahabi, V. R. Nafisi, and F. Pak, "Prediction of intradialytic hypotension using PPG signal features," 2015, pp. 399–404.
- [5] J. A. Kitterman, R. H. Phibbs, and W. H. Tooley, "Catheterization of umbilical vessels in newborn infants," *Pediatr. Clin. North Am.*, vol. 17, no. 4, Art. no. 4, 1970.
- [6] E. Chung, G. Chen, B. Alexander, and M. Cannesson, "Non-invasive continuous blood pressure monitoring: a review of current applications," *Front. Med.*, vol. 7, no. 1, Art. no. 1, 2013.
- [7] D. Buxi, J.-M. Redouté, and M. R. Yuce, "A survey on signals and systems in ambulatory blood pressure monitoring using pulse transit time," *Physiol. Meas.*, vol. 36, no. 3, Art. no. 3, 2015.
- [8] L. Peter, N. Noury, and M. Cerny, "A review of methods for non-invasive and continuous blood pressure monitoring: Pulse transit time method is promising?," *Irbm*, vol. 35, no. 5, Art. no. 5, 2014.
- [9] M. Kachuee, M. M. Kiani, H. Mohammadzade, and M. Shabany, "Cuffless blood pressure estimation algorithms for continuous health-care monitoring," *IEEE Trans. Biomed. Eng.*, vol. 64, no. 4, Art. no. 4, 2016.

- [10] G. Thambiraj, U. Gandhi, V. Devanand, and U. Mangalanathan, "Noninvasive cuffless blood pressure estimation using pulse transit time, Womersley number, and photoplethysmogram intensity ratio," *Physiol. Meas.*, vol. 40, no. 7, Art. no. 7, 2019.
- [11] T. Le *et al.*, "Continuous Non-Invasive Blood Pressure Monitoring: A Methodological Review on Measurement Techniques," *IEEE Access*, vol. 8, pp. 212478–212498, 2020, doi: 10.1109/ACCESS.2020.3040257.
- [12] C. Vlachopoulos, M. O'Rourke, and W. W. Nichols, *McDonald's blood flow in arteries: theoretical, experimental and clinical principles*. CRC press, 2011.
- [13] K. Chen, X. Zhang, Q. Zou, and X. Wang, "Individual-Based Cuffless Continue Estimation of Blood Pressure Measurement: Using Multiple Pulse Transmit Time," in *2020 International Conference on Intelligent Transportation, Big Data Smart City (ICITBS)*, Jan. 2020, pp. 889–892. doi: 10.1109/ICITBS49701.2020.00196.
- [14] Y. Chen, C. Wen, G. Tao, M. Bi, and G. Li, "Continuous and noninvasive blood pressure measurement: a novel modeling methodology of the relationship between blood pressure and pulse wave velocity," *Ann. Biomed. Eng.*, vol. 37, no. 11, Art. no. 11, 2009.
- [15] X. Ding, Y.-T. Zhang, J. Liu, W.-X. Dai, and H. Tsang, "Continuous Cuffless Blood Pressure Estimation Using Pulse Transit Time and Photoplethysmogram Intensity Ratio," *IEEE Trans. Biomed. Eng.*, vol. 63, Sep. 2015, doi: 10.1109/TBME.2015.2480679.
- [16] M. Kachuee, M. M. Kiani, H. Mohammadzade, and M. Shabany, "Cuff-less high-accuracy calibration-free blood pressure estimation using pulse transit time," 2015, pp. 1006–1009.
- [17] X.-R. Ding and Y.-T. Zhang, "Photoplethysmogram intensity ratio: A potential indicator for improving the accuracy of PTT-based cuffless blood pressure estimation," 2015, pp. 398–401.
- [18] Y.-L. Zhang, Y.-Y. Zheng, Z.-C. Ma, and Y.-N. Sun, "Radial pulse transit time is an index of arterial stiffness," *Hypertens. Res.*, vol. 34, no. 7, Art. no. 7, 2011.
- [19] M. R. Segal, "Machine learning benchmarks and random forest regression," 2004.
- [20] J. H. Friedman, "Stochastic gradient boosting," *Comput. Stat. Data Anal.*, vol. 38, no. 4, Art. no. 4, 2002.
- [21] C.-S. Kim, A. M. Carek, R. Mukkamala, O. T. Inan, and J.-O. Hahn, "Ballistocardiogram as Proximal Timing Reference for Pulse Transit Time Measurement: Potential for Cuffless Blood Pressure Monitoring," *IEEE Trans. Biomed. Eng.*, vol. 62, no. 11, pp. 2657–2664, Nov. 2015, doi: 10.1109/TBME.2015.2440291.
- [22] M. Radha *et al.*, "Estimating blood pressure trends and the nocturnal dip from photoplethysmography," *Physiol. Meas.*, vol. 40, no. 2, p. 025006, 2019.
- [23] F. Miao, Z.-D. Liu, J.-K. Liu, B. Wen, Q.-Y. He, and Y. Li, "Multi-sensor fusion approach for cuff-less blood pressure measurement," *IEEE J. Biomed. Health Inform.*, vol. 24, no. 1, pp. 79–91, 2019.
- [24] N. Ibtihaz and M. S. Rahman, "PPG2ABP: Translating Photoplethysmogram (PPG) Signals to Arterial Blood Pressure (ABP) Waveforms using Fully Convolutional Neural Networks," *ArXiv200501669 Cs Eess*, May 2020, Accessed: Aug. 08, 2021. [Online]. Available: <http://arxiv.org/abs/2005.01669>
- [25] Y. Dong, J. Kang, Y. Yu, K. Zhang, Z. Li, and Y. Zhai, "A Novel Model for Continuous Cuff-less Blood Pressure Estimation," in *2018 11th International Symposium on Communication Systems, Networks & Digital Signal Processing (CSNDSP)*, 2018, pp. 1–6.
- [26] A. Esmaili, M. Kachuee, and M. Shabany, "Nonlinear cuffless blood pressure estimation of healthy subjects using pulse transit time and arrival time," *IEEE Trans. Instrum. Meas.*, vol. 66, no. 12, pp. 3299–3308, 2017.
- [27] N. Agham and U. Chaskar, "Prevalent Approach of Learning Based Cuffless Blood Pressure Measurement System for Continuous Health-care Monitoring," 2019, pp. 1–5.
- [28] S. M. Anvari, M. Yazdchi, A. Kayvanpour, S. M. H. Nayeypour, T. Koivisto, and M. J. Tadi, "Design and implementation of a non-invasive and cuff-less arterial blood pressure monitoring system," 2017, pp. 1–4.
- [29] J. Shao, P. Shi, and S. Hu, "A Unified Calibration Paradigm for a Better Cuffless Blood Pressure Estimation with Modes of Elastic Tube and Vascular Elasticity," *J. Sens.*, vol. 2021, p. e8868083, Apr. 2021, doi: 10.1155/2021/8868083.
- [30] J. Zheng and Z. Yu, "A Novel Machine Learning-Based Systolic Blood Pressure Predicting Model," *J. Nanomater.*, vol. 2021, pp. 1–8, Jun. 2021, doi: 10.1155/2021/9934998.
- [31] I. Sharifi, S. Goudarzi, and M. B. Khodabakhshi, "A novel dynamical approach in continuous cuffless blood pressure estimation based on ECG and PPG signals," *Artif. Intell. Med.*, vol. 97, pp. 143–151, 2019.
- [32] S. M. Fati, A. Muneer, N. A. Akbar, and S. M. Taib, "A Continuous Cuffless Blood Pressure Estimation Using Tree-Based Pipeline Optimization Tool," *Symmetry*, vol. 13, no. 4, Art. no. 4, Apr. 2021, doi: 10.3390/sym13040686.
- [33] Y. Kurylyak, F. Lamonaca, and D. Grimaldi, "A Neural Network-based method for continuous blood pressure estimation from a PPG signal," in *2013 IEEE International Instrumentation and Measurement Technology Conference (I2MTC)*, May 2013, pp. 280–283. doi: 10.1109/I2MTC.2013.6555424.

- [34] G. Slapničar, N. Mlakar, and M. Luštrek, "Blood Pressure Estimation from Photoplethysmogram Using a Spectro-Temporal Deep Neural Network," *Sensors*, vol. 19, no. 15, Art. no. 15, Jan. 2019, doi: 10.3390/s19153420.
- [35] F. Miao *et al.*, "Continuous blood pressure measurement from one-channel electrocardiogram signal using deep-learning techniques," *Artif. Intell. Med.*, vol. 108, p. 101919, Aug. 2020, doi: 10.1016/j.artmed.2020.101919.
- [36] L. N. Harfiya, C.-C. Chang, and Y.-H. Li, "Continuous Blood Pressure Estimation Using Exclusively Photoplethysmography by LSTM-Based Signal-to-Signal Translation," *Sensors*, vol. 21, no. 9, Art. no. 9, Jan. 2021, doi: 10.3390/s21092952.